

THE ROLE OF NEW MRI TECHNIQUES IN THE DIAGNOSIS OF DIFFUSE LIVER DISEASES

Essay

Submitted for fulfillment of Master degree in Radiodiagnosis

By

Mohamed Ahmed Abd El Razek

M.B., B.Ch.

Faculty of Medicine Cairo University

Supervised By

Dr. Hany Ahmed Sami

Professor of Radiodiagnosis

Faculty of Medicine

Cairo University

Dr. Omar Moawia

Professor of Radiodiagnosis

Faculty of Medicine

Cairo University

Dr. Ahmed Abd El Samie

Lecturer of Radiodiagnosis

Theodor Bilharz Research Institute

FACULTY OF MEDICINE
EL KASR EL AINI - CAIRO UNIVERSITY

2012

Abstract

However, more clinical evidence is needed to determine which method or combination of methods achieves the best accuracy for assessment of fibrosis, fat, and iron deposition. In phase and opposed phase MR imaging allows reliable detection of focal steatosis hepatitis owing to the chemical shift cancellation artifact. Areas of steatosis demonstrate signal loss on opposed phase images. In addition, T2* effects allow reliable detection of iron storage diseases related susceptibility artifacts. Areas of iron storage demonstrate pronounced signal loss on the image with the longer echo time. MR spectroscopy has potential tool utility for assessment of metabolic function, particularly with respect to liver fat quantification. It also may provide useful information about other aspects of diffuse liver disease (eg, inflammation and fibrosis). However, in vivo application of MR spectroscopy in the abdomen and pelvis is limited by spectral resolution, SNR, and motion. In summary, MR spectroscopy of the liver is a novel evolving technology with the potential to improve tissue characterization when used in conjunction with other conventional MR sequences.

Key word: DIFFUSE LIVER DISEASES-MRI- *Radiodiagnosis*-
Haemochromatosis- Sarcoidosis- Hepatic steatosis

TO MY

MOTHER, FATHER

MY SISTER

And to my beloved ones

TO WHOM I AM OVERWHELMINGLY INDEBTED TO, THANK YOU AND GOD
BLESS YOU

ACKNOWLEDGMENTS

- First and foremost, I would like to give thanks to **ALLAH** the almighty.
- No words can express my feelings, great respect and deep gratitude for my Professor and tutor ***Prof. Dr. Essam Ali El Shiekh***, Professor of Diagnostic radiology, Faculty of Medicine, Cairo University, for his patience, continuous encouragement, invaluable guidance, constructive criticism and great support.
- I wish to express my deep gratitude to ***Prof. Dr. Hany Ahmed Sami***, Professor of diagnostic radiology, Faculty of medicine, Cairo University for accepting the idea of this work, his efforts and encouragement.
- I also extend my thanks and appreciation to ***Prof. Dr. Omar Moawia*** Professor of Diagnostic Radiology, Faculty of Medicine, Cairo University.
- It is my pleasure to express my deep appreciation to ***Dr. Ahmed Abd El Samie***, Lecturer of Diagnostic Radiology Theodor Bilharz research institute for his help, guidance and kind support.

LIST OF ABBREVIATIONS

ADC: Apparent diffusion coefficient
AO = aorta
CT = celiac trunk
CNR : Contrast to-Noise-Ratio
DA = duodenal artery
DWI: Diffusion weighted imaging
FLASH : Fast Low Angle Shot
Fl = falciforme ligament
Gd- DTPA : Gadolinium-Diethylene
Triamine Penta acetic Acid
HA = hepatic artery
HCV : Hepatitis C Virus
IVC : Inferior Vena Cave
LGA = left gastric artery
LHV : Left Hepatic Vein
LV = ligament venosum
LHA = left hepatic artery
LP : Left Portal Vein
MHV : Middle Hepatic Vein
MRI : Magnetic resonance imaging
MIP: Maximum intensity projection
RHA = right hepatic artery
RHV = right hepatic vein

RPV = right portal vein
SMA = superior mesenteric artery
SA = splenic artery
SMV = superior mesenteric vein
SV = splenic vein
PV : Portal Vein
SE : Spin Echo
SGE : Spoiled gradient echo
SI : Signal intensity
SNR : Signal to-Noise Ratio
SPIO : Super Paramagnetic Iron Oxide
SS : Single Shot
STIR : Short T1 Inversion Recovery
T : Tesla
TE : Time of Echo
TR : Time of Repetition
Turbo FLASH : Turbo fast low-angle shot
USPIO : Ultra small superparamagnetic iron
oxides
3D-GRE : Three Dimensional Gradient
Recalled Echo

LIST OF FIGURES

Figure 1: Segmentation of the liver.....	5
Figure 2: Axial maximum intensity projection (MIP) of the liver.....	6
Figure 3: 3D surface-shaded renderings MR images.....	8
Figure 4: Normal portal vein orientation and branching	8
Figure 5: Axial image MR images of the liver.....	9
Figure 6: Sagittal MR images of the liver.....	10
Figure 7: Coronal MR images of the liver.....	11
Figure 8: Normal MR images of the liver.....	12
Figure 9: Axial liver breath-hold images.....	19
Figure 10: Recommended liver MRI protocol.....	21, 22
Figure 11: Typical MR imaging examination of the liver.....	22, 23
Figure 12: Normal appearance of the liver at in-phase and opposed-phase MR imaging.....	24
Figure 13: Underlying physics of in-phase and opposed-phase imaging.....	25
Figure 14: Schematic diagram illustrates water molecule movement.....	26
Figure 15: The effect of a diffusion-weighted sequence on water molecules	27
Figure 16: Axial diffusion-weighted images.....	29
Figure 17: Graph of Signal intensity versus b values at diffusion-weighted imaging	30
Figure 18: Diagram shows metabolite frequency relative to water frequency.....	32
Figure 19: MR spectrum obtained in healthy liver	34
Figure 20: Uncorrected MR spectra obtained in liver.....	39
Figure 21: diffuse liver disease distribution.....	41
Figure 22: Haemochromatosis.....	42
Figure 23: Steatohepatitis.....	42
Figure 24: Glycogen Storage Disease.....	42
Figure 25: Segmental Fatty Liver.....	43
Figure 26: Liver Cirrhosis Caused by Viral Infection.....	43
Figure 27: Wilson's Disease weighted spin-echo.....	43
Figure 28: Wilson's Disease Gradient-echo.....	43
Figure 29: Sarcoidosis T2WIs MR image.....	44
Figure 30: Sarcoidosis Gadolinium-enhanced gradient-echo.....	44
Figure 31: Congested Liver.....	44
Figure 32: Microvesicular steatosis in the liver.....	46
Figure 33: Focal fatty sparing. Opposed-phase and corresponding in-phase images.....	50
Figure 34: Geographic steatosis hepatis.....	51
Figure 35: Axial breath-hold in-phase images.....	51
Figure 36: In-phase and out-of-phase images in two patients with hepatic steatosis.....	52
Figure 37: Schematic illustrates fat-water MR imaging.....	55
Figure 38: The correct placement of the MR spectroscopy voxel	57
Figure 39: Diagram shows the dominant lipid peaks in liver MR spectra.....	57
Figure 40: MR spectra show increasing size of lipid peaks relative to the water peak.....	58
Figure 41: Graphs illustrate the MR imaging spectra for a fatty liver.....	59
Figure 42: Graph summarizes MR imaging fat detection and quantification techniques...	60
Figure 43: The pericanalicular pattern of iron distribution	62
Figure 44: Postmortem liver from a patient with hereditary HC.....	63

Figure 45: Beta thalassemia post-mortem liver specimen	63
Figure 46: Cirrhotic liver biopsy with periportal sideronecrosis and iron deposition	63
Figure 47: Hemochromatosis versus transfusional siderosis.....	64
Figure 48: Hepatic iron deposition with cirrhosis.....	65,66
Figure 49: Patterns of signal dropout in iron overload.....	67
Figure 50: Dual imaging in a case with genetic hemochromatosis.....	69
Figure 51: Dual imaging in a case with genetic hemochromatosis.....	69
Figure 52: A case of biopsy proven hepatic iron overload and steatosis.....	70
Figure 53: Gross Micronodular cirrhosis.....	72
Figure 54: Incomplete septal cirrhosis.....	73
Figure 55: Drawings illustrate how the shape of a cirrhotic liver can be quite variable.....	73
Figure 56: Typical MRI findings in hepatic cirrhosis.....	75
Figure 57: MR appearances of Fine nodular architecture in liver cirrhosis.....	77
Figure 58: Chronic hepatitis C without evidence of fibrosis at liver biopsy.....	79
Figure 59: 46-year-old man with chronic hepatitis C viral cirrhosis.....	81
Figure 60: Porto-venous phase coronal MIP MR image of Budd Chiar.....	86
Figure 62: Contrast-enhanced three-dimensional MR portography.....	86
Figure 63: Portal venous phase coronal source MR.....	87
Figure 64: Sarcoidosis in Liver	89
Figure 65: 63-year-old woman with liver lesions in sarcoidosis.....	90

Contents

<i>Titles</i>	<i>Page No.</i>
Introduction.....	1
Chapter 1: MRI Anatomy of the Liver.....	4
Chapter 2: MR imaging techniques of the liver	13
A) Conventional Techniques.....	16
B) Advanced MRI Techniques.....	23
Chapter 3: Diffuse liver diseases pathology and MR imaging Findings.....	41
i. Hepatic steatosis.....	45
ii. Haemochromatosis.....	61
iii. Hepatic Cirrhosis.....	71
iv. Budd-Chiari Syndrome.....	84
v. Sarcoidosis.....	88
Summary.....	92
References	
Arabic Summary	

INTRODUCTION

Introduction

MRI plays an increasingly important role for assessment of patients with chronic liver disease. MRI has numerous advantages, including lack of ionizing radiation and the possibility of performing multiparametric imaging. With recent advances in technology, advanced MRI methods such as diffusion, chemical shift based fat-water separation and MR spectroscopy can now be applied to liver imaging. *(Taouli et al, 2009)*

Magnetic resonance (MR) imaging has role in evaluation of diffuse liver disease. Hepatic MR imaging has been proved to be a comprehensive modality for assessing the morphology and functional characteristics of the liver. Concurrent technical improvements as well as implementation of advanced imaging sequence designs permit high-quality examination of the liver with T1-, T2-, and diffusion-weighted pulse sequences. Three basic demands remain if MR imaging is chosen for hepatic imaging: to improve parenchymal contrast, to suppress respiratory motion, and to ensure complete anatomic coverage. *(Boll and Merkle et al, 2009)*

A T1-weighted gradient-echo in-phase and opposed-phase sequence has become a routine part of every hepatic magnetic resonance (MR) imaging protocol. Although this sequence is primarily used to identify common pathologic conditions, such as diffuse or focal steatosis and focal fatty sparing, it is also helpful in detection of pathologic entities associated with T2* effects owing to the double-echo approach. A complete understanding of both the chemical shift cancellation artifact and the T2* effects of the in-phase and opposed-phase sequence is important for correct interpretation of hepatic MR images. *(Merkle and Nelson, 2006)*

Diffusion-weighted imaging is an evolving technology with the potential to improve tissue characterization when findings are interpreted in conjunction with findings obtained with other conventional MR imaging sequences. *(Qayyum, 2009)*

Diffusion weighted echo planar imaging, an adaptation from neuroimaging, is fast becoming a routine part of the MRI liver protocol to improve lesion detection and characterization of liver lesions. (*Maniam S et al, 2010*)

Magnetic resonance (MR) spectroscopy allows the demonstration of relative tissue metabolite concentrations along a two or three dimensional spectrum based on the chemical shift phenomenon. MR spectroscopy of the liver is an evolving technology with potential for improving the diagnostic accuracy of tissue characterization when spectra are interpreted in conjunction with MR images. (*Qayyum, 2009*)

The basic pathophysiology of diffuse parenchymal hepatic diseases usually represents a failure of metabolic pathways. Specific parenchymal diseases can be categorized as **storage, vascular, and inflammatory diseases**. (*Boll and Merkle et al, 2009*)

Noninvasive detection and **quantification of fat** is becoming more and more important clinically. Magnetic resonance (MR) imaging based techniques including chemical shift imaging, frequency-selective imaging, and MR spectroscopy are currently in clinical use for the detection and quantification of fat-water admixtures, with each technique having important advantages, disadvantages, and limitations. These techniques permit the breakdown of the net MR signal into fat and water signal components, allowing the quantification of fat in liver tissue, and are increasingly being used in the diagnosis, treatment, and follow-up of fatty liver disease. (*Hughes Cassidy et al, 2009*)

Magnetic resonance (MR) imaging is the most sensitive and specific imaging modality in the diagnosis of **hemochromatosis**. The susceptibility effect caused by the

accumulation of iron leads to signal loss in the affected tissues, particularly with the T2*-weighted sequences, which makes the diagnosis of iron overload possible. By using MR imaging techniques, it is possible to estimate the hepatic iron concentration in a noninvasive way, thereby avoiding repeated biopsies. (*Queiroz-Andrade et al, 2009*)

Patients with **chronic hepatitis B and hepatitis C virus** infections are at high risk of development of hepatic fibrosis and cirrhosis. In chronic viral hepatitis, evaluation of disease severity and the indications for antiviral therapy usually rely on histologic findings obtained at liver biopsy performed to assess degree of fibrosis. The sensitivity of conventional MRI in the detection of liver fibrosis and early cirrhosis is limited, and noninvasive imaging techniques have not yet been definitely established for the detection of liver fibrosis. With diffusion-weighted MRI (DWI) water diffusion is quantified by calculation of the apparent diffusion coefficient (ADC), which can be used to quantify liver fibrosis in patients with chronic liver disease. (*Taouli et al, 2007*)

The aim of work

Embracing the role of new MRI techniques as diffusion, chemical shift as well as spectroscopy together with the conventional MRI techniques in tissue characterization, diagnosis and staging of diffuse liver diseases for better impact on the treatment as well as prognosis.

MRI ANATOMY OF THE LIVER

Magnetic resonance (MR) imaging provides comprehensive evaluation of the liver including the parenchyma, biliary system, and vasculature. While computed tomography and sonography are often the initial studies used in evaluating the liver, MR is increasingly relied upon as a primary imaging modality in addition to its problem-solving capacity. MR provides soft tissue characterization unachievable with other imaging modalities. Lack of ionizing radiation and relative lack of operator dependence are additional advantages over computed tomography and ultrasound respectively. Moreover, it enables the radiologist to take axial, sagittal and coronal images when evaluating the liver. Rapid breath-hold pulse sequences have largely replaced older, slower pulse sequences, resulting in shortened examination times. *(Fisher et al, 2005)*

The major vascular structures are most consistently demonstrated in the axial MR images. With spin echo MRI, generally vessels are delineated as areas of signal void. *(Robinson et al, 2006)*

A wide range of protocols are available due to numerous combinations of field strength, pulse sequence implementation and interdependent sequence parameters, all of which can confluence image quality. *(Lomas, 2008)*

Segmental anatomy:

The eight liver segments are numbered clockwise based on frontal view of the liver, beginning with the postero-superior segment of the left paramedian sector, which corresponds to the caudate lobe, and ending with segment VIII which is consistent with the postero-superior segment of the right paramedian sector **(Fig.1)**. *(Schneider, 2006)*

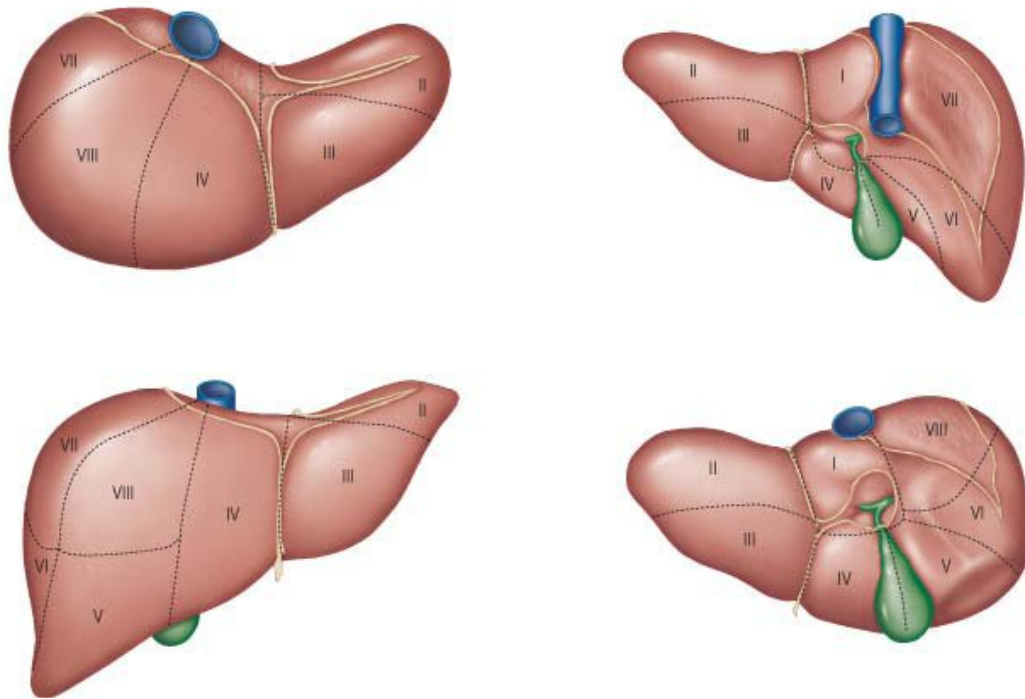


Fig.1: Showing Segmentation of the liver. (*Standring et al, 2005*)

Anatomically, the borders of the liver segments are well-defined, but show a wavy shaped course. However, in clinical routine, segmentation of the liver in cross sectional MR imaging is sharply demarcated and usually based on certain landmarks that define the underlying borders. (*Lee et al, 2007*)

Based on these landmarks, the IVC is considered the center point for liver segmentation. A line from the IVC to the middle hepatic vein and the gall bladder separates the left and right hemi liver and the corresponding liver segments V/VIII and I/IV (a & b) respectively. Whereas the axis between the IVC and right hepatic vein corresponds to the border between liver segments VI/VII and V/VIII, the line between the IVC and left hepatic vein and the falciform ligament separates liver segments IV a and IV b from segments II and III. (*Schneider, 2006*)

Whereas liver segments VII, VIII, I, IV a and II are located at the posterior aspect of the imaged abdominal situs and above the level of the left and right main portal vein, segments VI, V , IVb and III are located inferior to the level of main portal veins

at the anterior aspect of the liver. Segment I corresponds to the caudate lobe as shown in (Fig.2). (Shahid, 2007)

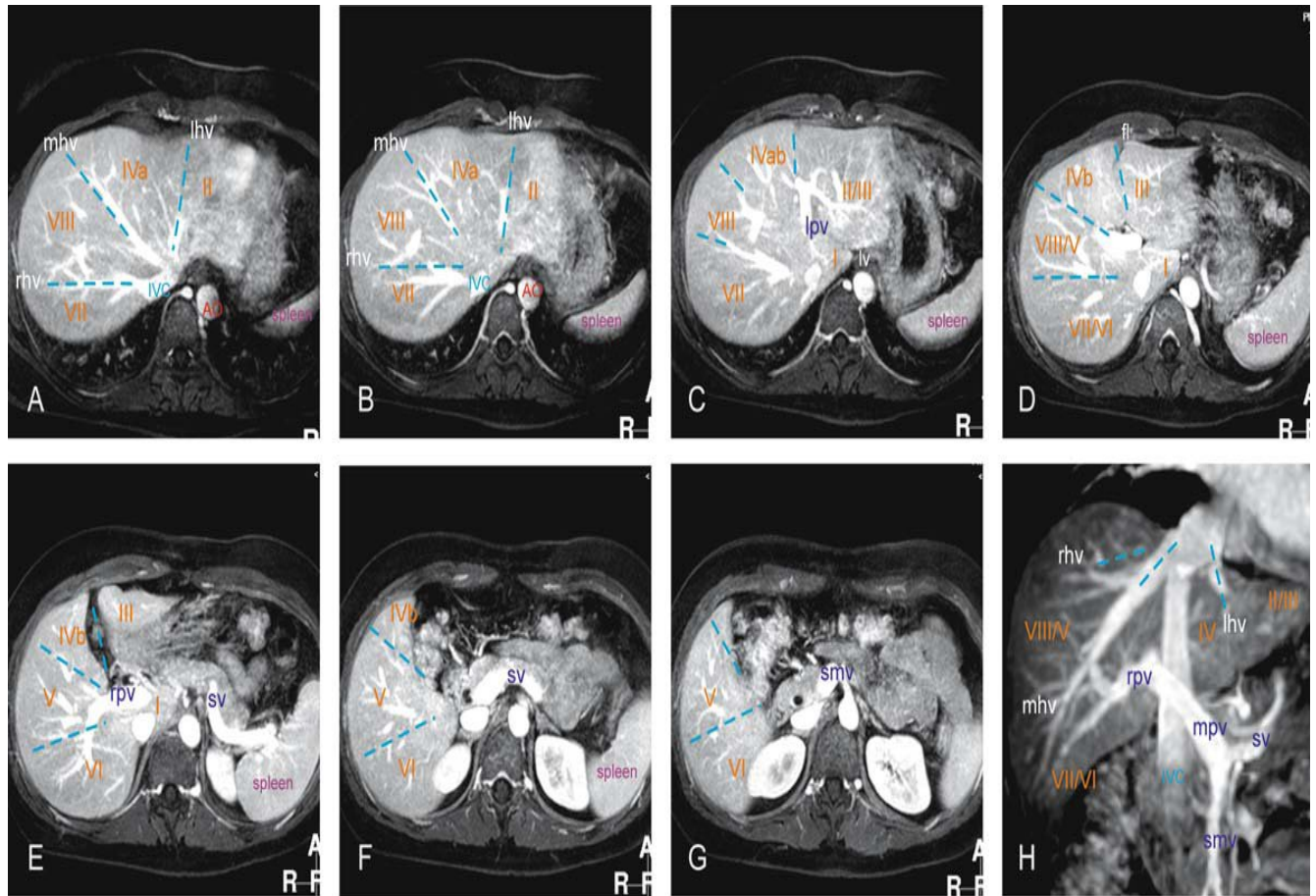


Fig.2: A–G Axial maximum intensity projection (MIP) based on the three-dimensional (3D) gadolinium-enhanced delayed phase gradient echo images at various levels shows the hepatic segments (I–VIII), three hepatic veins, portal vein, and ligaments. H. Coronal reformat shows the relationship among the hepatic segments, three hepatic veins, portal vein (formed by the splenic and superior mesenteric veins), and inferior vena cava. (Shahid, 2007)

Vascular anatomy:

Normal hepatic arterial supply occurs only in a small majority of subjects. In 55% of cases, the common hepatic artery (CHA) gives rise to the right hepatic artery (RHA), middle hepatic artery (MHA), and left hepatic artery (LHA) (114.1J); in 11%, the RHA originates from the superior mesenteric artery (SMA); in 10%, a replaced LHA is present; in 8% the RHA, MHA, and LHA arise from the CHA with an accessory LHA from the left gastric artery (LGA); in 7%, the RHA, MHA, and LHA arise from the CHA with an accessory RHA from the LGA; and in 4.5%, the entire CHA